ROBUST ANALYSIS AND CONTROL DESIGN OF THE HEAD-NECK SYSTEM

By

Andrey L. Maslennikov

A THESIS

Submitted to
Michigan State University
in partial fulfillment requirements
for the degree of

Mechanical Engineering – Master of Science

2013

ABSTRACT

ROBUST ANALYSIS AND CONTROL DESIGN OF THE HEAD-NECK SYSTEM

By

Andrey L. Maslennikov

Neck pain is the one of the most frequently reported musculoskeletal complaints. A systematic evaluation of a neck condition may allow clinicians to diagnose possible problems that a subject might have in an objective manner. In this dissertation, we propose a systematic methodology for measuring robustness of the head-neck system that can be used as an objective measure of the head-neck system characteristics. Our method builds on computing the structured singular value μ as a measure of robustness for a particular subject. The μ value is computed under the consideration that the variability of head-neck system model parameters for a tested subject comes from the estimation errors as well as from the natural variation of biological parameters. Both sources of subject's variability determine uncertainty levels that are within some physiologically reasonable ranges. In addition, we analyzed worst-case scenarios of the head-neck system model. The worst-case analysis can provide us with a possible tool to predict what would be the combination of parameters that may cause the worst-case performance. Finally, the design of the robust controller for the head-neck system is also discussed in this dissertation.

ACKNOWLEDGMENTS

I would like to extend my sincere gratitude to my adviser Dr. Jongeun Choi, who led me through my whole M.S. program. I would like to acknowledge faculty members with whom I worked for the last two years: Dr. Clark Radcliffe from Mechanical Engineering Department, Drs. Jacek Cholewicki, Peter Reeves, John Popovich from College of Osteopathic Medicine. Very special thanks to my lab-mate Cody Priess. I also want to say thank you to my best friends Pavel Polunin and Oleksii Karpenko who supported me all these years and also all my other friends at Michigan State University.

Finally, this work has been supported in part by grant number U19 AT006057 from the National Center for Complementary and Alternative Medicine (NCCAM) at the National Institutes of Health.

TABLE OF CONTENTS

LIST OF TABLES

LIST OF FIGURES

1 Introduction

One of the most frequently reported musculoskeletal complaints is neck pain [Côté et al., 1998], [Holmström et al., 1992]. The current method of evaluation is primarily based on (subjective) surveys from subjects; see [Langley and Sheppeard, 1985]. Hence, researchers have been working on developing an objective evaluation of neck pain subjects and classification of subjects between control and pain groups. Such measure can yield a numerical value, which may estimate and/or predict conditions of the head-neck system. Our motivation is to develop a rigorous procedure of computing such objective measure.

A mathematical description of the head-neck system, as a dynamical system, can be described as an interconnection of transfer functions including an internal controller, muscle dynamics, plant dynamics (skeleton with ligaments), and neurological delays. Previous studies proposed different models of the head-neck system dynamics, for example, [Hannaford et al., 1986], [Huebner et al., 1992], [Peterson et al., 2001], and [Chen et al., 2002]. In this dissertation we adopt a model with a fixed structure developed in [Priess et al., 2012]. In their study, performance of the head-neck system was investigated during a tracking task, where participants were asked to follow a moving target using a custom-made head-mounted laser device. Parameters of the developed model were estimated from time series data produced by a target trajectory as an input and a laser dot trajectory as an output. The estimated model showed good fitting that makes it applicable to our studies.

It should be noted that a fixed low-order linear model structure may neglect nonlinear and/or high-order dynamics of the system that may result in modeling errors. In addition, such models do not take into account a discrete decision making process that a subject may have, which results in hybrid systems. Furthermore, parameters of the head-neck system could vary within some physiological ranges due to, for instance, fatigue, task assignment, control strategy and so on; see [Davids et al., 2006] and [Newell and Corcos,

1993]. Moreover, parameters of the head-neck system are not known and, consequently, these parameters should be estimated using system identification techniques discussed in [Ljung, 1999], [Forssell and Ljung, 1999], and [Gustavsson et al., 1977]. Assuming the system is time-invariant, the estimated parameters using a finite number of observations will have estimation errors. Therefore, in addition to the biological variability in system parameters, the estimation errors need to be also taken into account when analyzing stability and/or performance of the head-neck system.

From an engineering perspective, one of the most important questions is whether or not the dynamical system is stable. On the other hand, from a medical point of view, mathematical instability of the head-neck model could be related to an injury. By considering a set of all possible models due to the biological variability and parameter estimation errors we need to investigate robust stability of an uncertain model rather than of stability of a single true (nominal) model. Robust stability tests deal only with system's internal behavior assuming no existence of any external excitation. On the other hand, humans aim to control their dynamics under the influence of external inputs/commands as can be seen in position-tracking tasks. Robust performance analysis may be used to investigate how a dynamical system attenuates the signals of the performance channels from exogenous influences in spite of uncertainties. In addition, robust performance analysis may help us to classify subjects between control and pain groups as we will show further. Robust stability and robust performance analyses of the head-neck system with respect to its total variability could provide us with objective evaluations of the head-neck system.

There exist previous attempts to conduct robust analysis of human dynamics. The robustness of a human postural control system focusing on stability margins under impulsive perturbations was analyzed in [Hur et al., 2010]. The robust space of a PD controller structure of a human postural control system was investigated in [Masani et al., 2006]. A methodology of designing an optimal control for postural systems was proposed in [Xu et al., 2010]. However, in those studies uncertainties either in a model or estimated sys-

tem parameters were not considered. Therefore, it is crucial to develop a new approach of measuring robustness of the head-neck system with respect to a set of all possible models for a particular subject. In the past, an estimated system was considered to be the true nominal system, and the stability analysis was then followed on the estimated system. There has been no effort to gauge uncertainties in such systems from experimental data in order to analyze stability and performance.

The stability and performance analyses of systems subjected to structured uncertainties can be addressed with the structured singular value, μ [Zhou and Doyle, 1998]. The μ value can be used as a measure of system's robust stability and robust performance. Robust control theory and μ analysis are described in [Skogestad and Postlethwaite, 2005], [Zhou and Doyle, 1998], [Balas et al., 2001], and [Balas et al., 2006]. Computing the μ value with the exact combination of system parameters that will yield the worst-case performance for a given set of models, is also important. From a medical point of view, analyzing such worst-case performance and its associated parameters for a given subject could provide the worst-case scenario, which the subject should avoid.

The contributions of this dissertation are as follows. We provide a description of the proposed methodology for evaluating subjects' head-neck system in an objective manner. In comparison to approaches based on surveys [Langley and Sheppeard, 1985], our measure will be objective. To begin with, we describe the experimental setup that is used to collect data from subjects for a head-neck position-tracking task. We then show how the parameters of the head-neck system model can be estimated using nonlinear least squares optimization by minimizing the difference between the actual subject's response and the simulated model response. With a set of estimated parameters for each subject we present a way to compute biological, estimation, and, eventually, subject's total parameter variabilities. Due to variability in parameters the dynamics of the head-neck system are described by a set of dynamical models for which a robust analysis should be applied. We define necessary criteria for the robust analysis of the head-neck system based on the $\mathcal{H}_\infty$

norm of the sensitivity function. For the robust performance analysis we incorporate the performance weighting function, which is used to define a boundary between satisfactory and not satisfactory performance. Further, we give an interpretation of the μ value as an objective measure of the head-neck system's condition. Using the μ value we analyze which block which individual parameter of the head-neck system are critical to system's robust performance. Then we use the worst-case robust analysis to show how a likelihood of being injured for a tested subject can be suggested. Finally, we describe the robust control of the head-neck system that possibly can be used as a guideline for physical therapists in developing treatment for patients. In order to show the applicability of the proposed methodology we perform all aforementioned analyses for experimentally obtained data from 5 subjects. The computed μ values allow us to see similarities and differences among subjects.

The remainder of this dissertation is organized as follows. Chapter 2 provides a description of the head-neck system with uncertainties. In Chapter 3 we describe an experimental setup that we use for collecting data from subjects and an estimation process of the head-neck model parameters and describe how the biological, estimation and total subject variabilities could be obtained. In Chapter 4 we briefly review criteria for robust stability and robust performance of the system for our further analyses. In Chapter 5 we show which components (control, muscle dynamics, plant dynamics or delays described in Chapter 2) of the head-neck system are most critical to robust stability and robust performance of the system. In Chapter 6 we investigate how each individual parametric uncertainty affects robust stability and robust performance of the head-neck system. The worst-case analysis of the head-neck system is presented in Chapter 7. The design of a robust controller with a fixed structure for the head-neck system model is discussed in Chapter 8. Finally, we provide concluding remarks in Chapter 9.

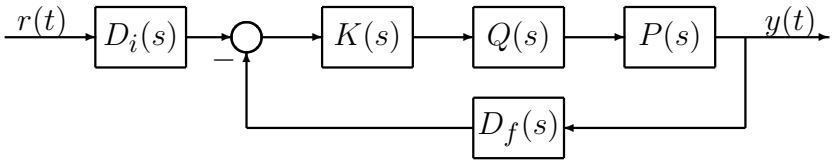

Figure 1: Head-neck system model.

2 Head-neck System Model Description

In this chapter we provide a description of the head-neck system model. A variety of the head-neck system models exist. For example, a sixth-order nonlinear model was used in [Hannaford et al., 1986] and smooth pursuit of an eye-head tracking system with their own model was analyzed in [Huebner et al., 1992]. We adopt a model from [Priess et al., 2012] considering the good fit to preliminary experimental data. This model can be used to represent head-neck dynamics in both flexion/extension and axial rotation. To simplify the presentation, we investigate only flexion/extension case. However, the exact same approach can be applied to the axial rotation case in a straightforward manner.

Our model, shown in Fig. 1, contains a neurological (visual) delay in the input channel and a follow-up closed-loop subsystem. This subsystem contains a controller, muscle dynamics, and plant (skeleton and ligaments) dynamical blocks in the forward loop and a neurological delay in the feedback channel. Each component of the head-neck system can be represented by a transfer function in the s-domain; see [Skogestad and Postlethwaite, 2005]. Here we denote the neurological delay in the input channel by $D_i(s)$, the controller by $K(s)$, muscle dynamics by $Q(s)$, plant dynamics by $P(s)$, and the neurological delay in the feedback channel by $D_f(s)$.

The neurological delays, as a part of postural control system, were already considered in previous works. For example, the step response of eye motion and the neurological (visual) delay in the input channel were analyzed in [Carl and Gellman, 1987]. The delay in the input channel as a component of the head-neck system model is also mentioned in [Peterson et al., 2001] and [Chen et al., 2002]. A neurological delay in the forward

loop of the head-neck system model and the corresponding time constant were considered in [Robinson et al., 1986]. The existence of the delay in the feedback channel is also mentioned in [Masani et al., 2006]. Note that for computational simplicity, we used a first-order Padé approximation for delays, but a higher-order approximation could also be used.

The controller $K(s)$ is assumed to have a fixed PID structure. A PID or PD controller structure is one of the most popular choices for studies in postural control. For example, a PD controller was used to simulate human posture control in [Masani et al., 2006]. $Q(s)$ is modeled by a first-order transfer function and its structure was proposed in [Peterson et al., 2001] and [Chen et al., 2002].

Plant dynamics, $P(s)$, is represented by a second-order transfer function and it was used in [Peng et al., 1996], [Chen et al., 2002], and [Robinson et al., 1986]. The values of stiffness and damping ratio were experimentally obtained in [Bourdet and Willinger, 2008] and [Pankoke et al., 1985]. Plant dynamics, by considering the structure of the skeleton, was analyzed in [Reber and Goldsmith, 1979] and [Vette et al., 2011].

Finally, the described blocks of the head-neck system, in terms of transfer functions, are defined as follows.

$$\begin{aligned} D_i(s) &= e^{-\tau_i s} \approx \frac{2-\tau_i s}{2+\tau_i s}, \\ D_f(s) &= e^{-\tau_f s} \approx \frac{2-\tau_f s}{2+\tau_f s}, \\ K(s) &= K_p + K_d s + \frac{K_i}{s}, \\ Q(s) &= \frac{1}{\tau_m s + 1}, \\ P(s) &= \frac{1}{I s^2 + b s + k}, \end{aligned} \tag{1}$$

and the closed-loop transfer function $M(s)$ of the head-neck system model as follows.

$$M(s) = D_i(s)\frac{K(s)Q(s)P(s)}{1 + K(s)Q(s)P(s)D_f(s)}. \tag{2}$$

3 Parameter Estimation

The parameters of the head-neck system model should be estimated. In order to estimate these parameters a physical experimental setup for the position-tracking task was constructed. In this experimental setup a tested subject sit on the chair in front of the screen. A projector was placed above a tested subject and the laser was rigidly mounted on subject's head. During this position-tracking task, an individual subject was asked to follow a projected cross on the screen in front of the subject with a dot from a laser on the head. Positions of both dots were calculated from images captured by a video camera and saved as to time series data. The experimental procedure and setup was described in detail previously in [Priess et al., 2010]. The diagram of the experimental setup is presented in Fig. 2.

In our particular case, five healthy subjects signed their informed consent form and participated in the experiments. Each individual subject completed five trials of a position-tracking task on two different days. This experimental procedure was approved by the Michigan State University Biomedical and Health Institutional Review Board (IRB# 12-456).

Parameters of the head-neck system model were estimated using these time series data sets for each trial independently. Each estimation provides us with a vector of estimated parameters $\hat{\theta}$, which has the following structure

$$\hat{\theta} = [\hat{K}_p, \hat{K}_d, \hat{K}_i, \hat{\tau}_m, \hat{I}, \hat{b}, \hat{k}, \hat{\tau}_f, \hat{\tau}_i]^\top \in \mathbb{R}^9, \tag{3}$$

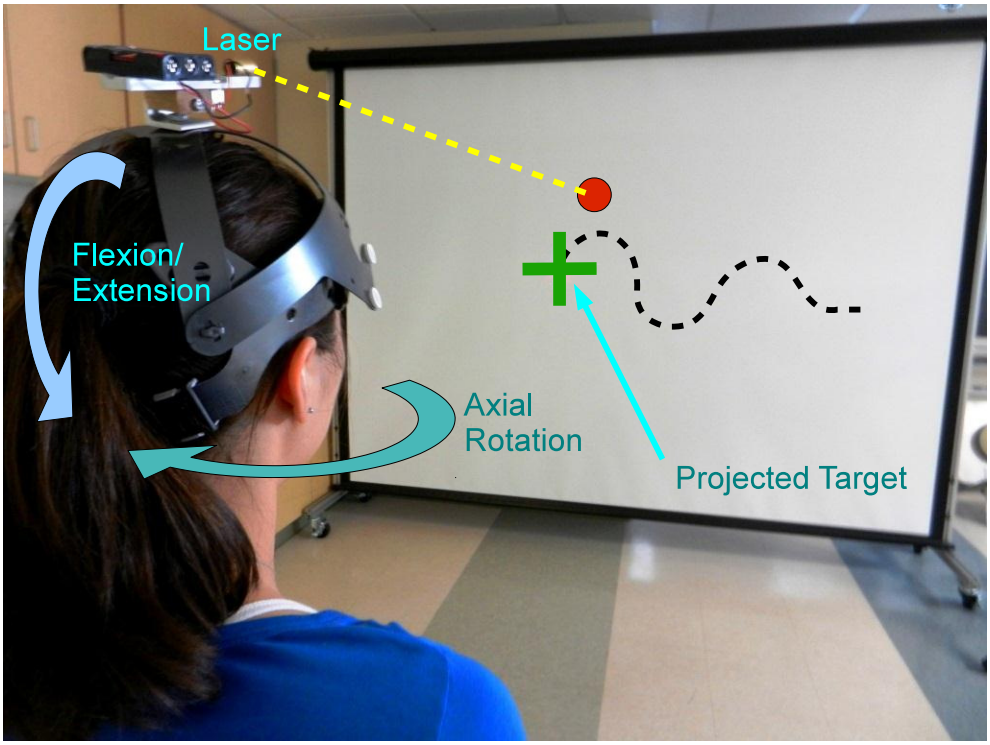

Figure 2: The experimental setup of a head-neck position-tracking task. Adapted from [Priess et al., 2012]. (For interpretation of the references to color in this and all other figures, the reader is referred to the electronic version of this thesis.)

where the inertia parameter I, is computed using subject's weight with methods described in [Winter, 2004] and [Yoganandan et al., 2009].

The parameter vector θ is estimated using the experimental input and output data. Based on our preliminary studies, a pulse-width modulated (PWM) signal was chosen as an input type for our experiments. The time between signal changes varied from 0.3 to 0.9 seconds randomly with a normal distribution in order to eliminate the predictability aspect. In this way, we eliminate any feed-forward actions in the closed-loop system while focusing on feedback mechanism. Another reason of using a time-varying step function is to generate the signal with a desired frequency spectrum, as can be seen from Fig. 3. The desired frequency spectrum of the input signal should be such that it covers the bandwidth of the head-neck system, which is about 1 Hz, according our preliminary

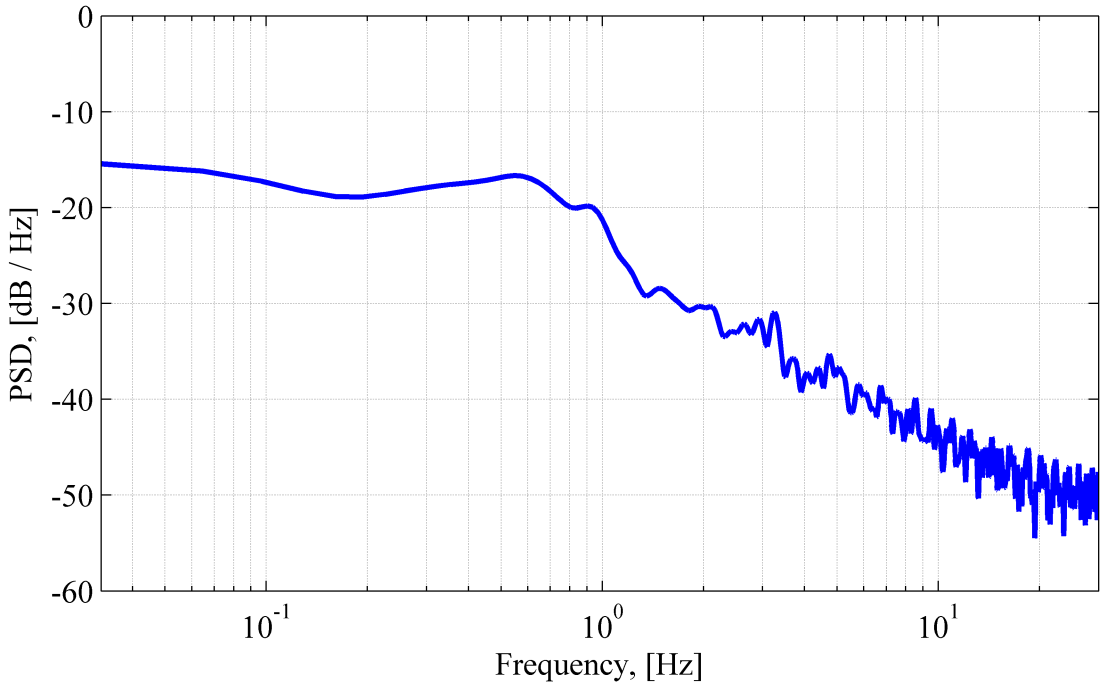

Figure 3: Power spectral density of the input signal.

studies. The output signal is the actual subject's response during the position-tracking experiment. Both input and output signals were simultaneously captured by a video camera at frequency 60 Hz in order to remove any delays in the projection.

The parameter vector θ is estimated based on nonlinear least-square optimization. It's description can be found in [Levenberg, 1944], [Marquardt, 1963], and [Dennis Jr., 1977]. In our case, we are looking for such vector θ within a set Θ that minimizes the difference between the experimentally obtained subject's response Y and the simulated subject's response $F(\theta)$. In other words, vector $\hat{\theta}$ contains the parameters such that the simulated response $F(\hat{\theta})$ fits best to the actual subject's output Y. Mathematically this method can be described as follows.

$$\hat{\theta} := \arg\min_{\theta \in \Theta} \|F(\theta) - Y\|_2^2, \tag{4}$$

where Θ is a compact set whose element-wise boundaries are defined by the parameter-wise variability of vector θ over the whole population. In other words, the set Θ includes

all physiologically possible parameters of the head-neck system model.

To perform the robust analysis we need to characterize uncertainties in system parameters. In our case, each parametric uncertainty is within a range defined by the biological and estimation variabilities. In order to determine the subject's biological variability, we perform a set of experimental trials. The parameters of the head-neck system model are estimated using data from each individual trial. Furthermore, n denotes the number of trials, which in our experiments is 10 for each subject. Having a set of ten vectors $\hat{\theta}$, we compute three vectors: $\hat{\theta}_{avg}$, $\hat{\theta}_{min}$, and $\hat{\theta}_{max}$. $\hat{\theta}_{avg}$ is the vector with the average values of the estimated parameters, and $\hat{\theta}_{min}$ and $\hat{\theta}_{max}$ defines the boundaries of the estimated parameters or the element-wise ranges in which the parameters of the head-neck system could vary for a tested subject due to the biological variability. Here and further, index i, such that $i \in \mathcal{I} := \{1, \cdots, n\}$, denotes the number of trial and index j, such that $j \in \mathcal{J} := \{1, \cdots, 9\}$, denotes a particular element in $\hat{\theta}$. The parameter vector $\hat{\theta}_{avg}$ determines the nominal model. These three vectors are defined as follows.

$$\begin{aligned} \hat{\theta}_{avg} &= \mathop{\mathbb{E}}_{i \in \mathcal{I}}[\hat{\theta}^i], \\ \hat{\theta}_{j\ min} &= \min_{i \in \mathcal{I}}(\hat{\theta}^i_j), \\ \hat{\theta}_{j\ max} &= \max_{i \in \mathcal{I}}(\hat{\theta}^i_j) \end{aligned} \tag{5}$$

The total subject's variability is defined as a union of the biological and estimation variabilities. To this end, we also consider the estimation error for a given set of estimated parameters of a subject. To compute the total subject's variability we perform the Monte-Carlo simulations, where for each estimated $\hat{\theta}^i$ we simulate the model, as shown in Fig. 4, $N = 50$ times with different realizations of additive white noise in muscles. The parameters of the model are estimated for each Monte-Carlo simulation. Using the whole set of these estimates the parameter-wise boundaries (vectors $\hat{\theta}_{min,\ tot}$ and $\hat{\theta}_{max,\ tot}$) of the estimates are computed in a same way as it was done for the biological variability

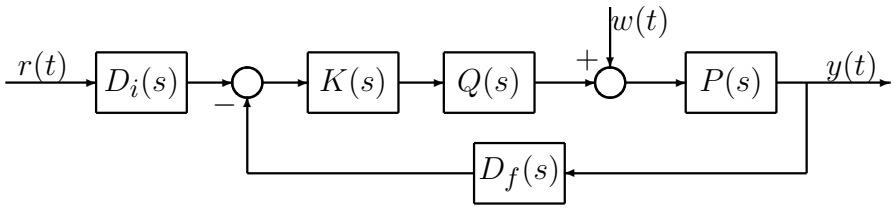

Figure 4: Head-neck system model for Monte-Carlo simulations

using Eq. (5).

These two vectors $\hat{\theta}_{min,\ tot}$ and $\hat{\theta}_{max,\ tot}$, which are parameter-wise boundaries, form a compact set Θ_{subj} uniquely for an individual subject. Finally, the total subject's variability is defined as follows.

$$\hat{\theta} \in \Theta_{subj}, \text{ with some probability } \alpha \tag{6}$$

where the associated probability α can be obtained from Θ_{subj} and the estimation error statistics.

Since our estimation is based on signal statistics and randomness in human behavior, the vector of the estimated parameters $\hat{\theta}$ and the whole set Θ_{subj} are estimated with some probability α as in Eq. (6). Additionally, the natural description of the uncertainty level for the estimation error variability can be made more explicitly for the robust stability and performance analyses. This aspect was investigated in [Ljung, 1999], [Bombois, 2000], [Bombois et al., 2001], and [Gevers et al., 2003]. According to those studies, the estimated parameter $\hat{\theta}$ lies in the ellipsoidal uncertainty region U_{ol} with some probability $\alpha(q, \chi) = Pr(\chi^2(q) < \chi)$, where $\chi^2(q)$ the chi-square distribution with q parameters. The ellipsoidal uncertainty region U_{ol} defined as follows.

$$U_{ol} = \{\theta | (\theta - \hat{\theta})^\top P_\theta^{-1} (\theta - \hat{\theta})^\top < \chi\}, \tag{7}$$

where P_θ is the covariance matrix of $\hat{\theta}$, which is different from the formulation in Eq. (6).

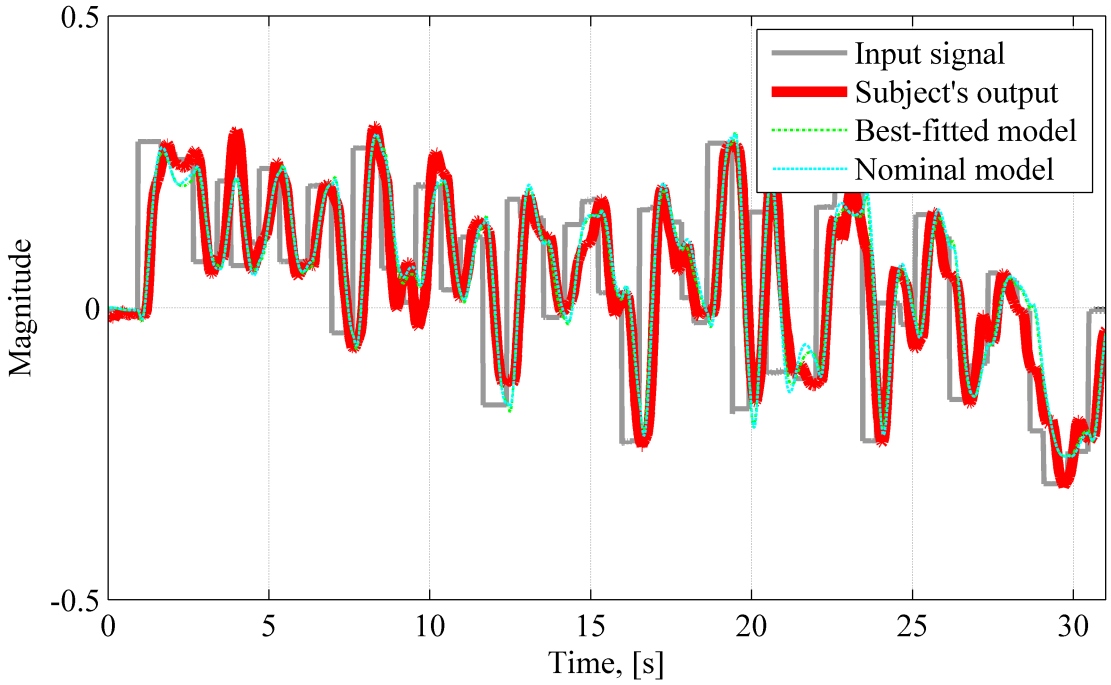

Figure 5: Input and output data collected from subject 1 and the response of the estimated model.

The estimated nominal parameters for each subject as well as its biological and total variabilities are listed in three tables presented in Appendix A. An example of the input signal and actual subject's response with the best fitted simulated response is presented in Fig. 5. As can be noted, the simulated response (green dashed line) of the model with the set of fitted parameters $\hat{\theta}^1$ and the simulated response of the nominal model (cyan dashed-dotted line) are close to the actual subject's response at trial 1. This means that the model structure with the estimated parameters allows us to capture dynamics of the system. Nevertheless, small deviations between the simulated response and the actual subject's output, caused by the estimation and modeling errors, could be observed.

In general, we observed some general trends in the estimated parameters from subjects. However, estimates for subject 5 are not consistent with others and the total variability for that subject is higher than those of others. The results of Monte-Carlo simulations for subject 5 are shown in Fig. 7. From this figure it could be noted that a set of simulated

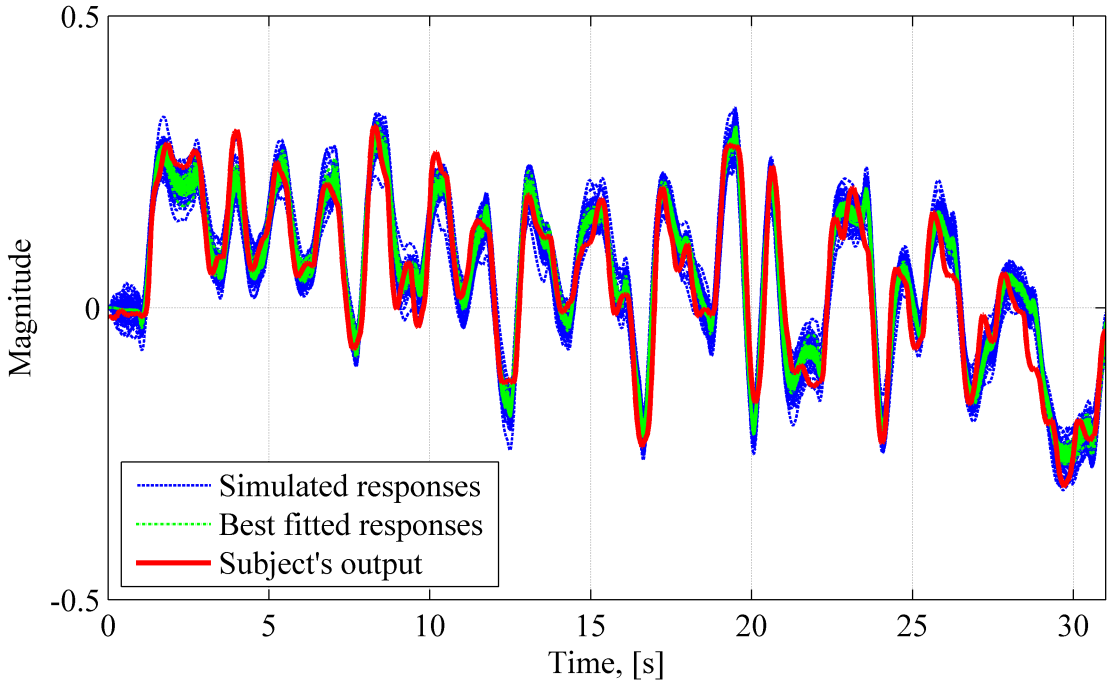

Figure 6: Monte-Carlo simulations for the estimated model for trial 1, subject 1.

responses as well as a set of fitted models are not so close to the actual subject's response for subject 5 in comparison to the case of subject 1 (see Fig. 6). Such deviations can be caused by error and uncertainty in modeling.

4 Robust Stability and Performance Criteria

An important question in analysis and control design of dynamical systems is about stability of these systems. However, with the presence of uncertainties in a dynamical system the robust stability analysis has to be involved. Robust stability is stability of an uncertain dynamical system with respect to a set of all uncertainties specified for that dynamical system. To answer this question, a dynamical system has to be transformed to the form presented in Fig. 8 a) where $G(s)$ is the generalized plant and Δ_{st} is the uncertainty matrix. In our case all uncertainties are parametric, in other words, structured, and; consequently, the matrix Δ_{st} is block diagonal uncertainty matrix. Taking an

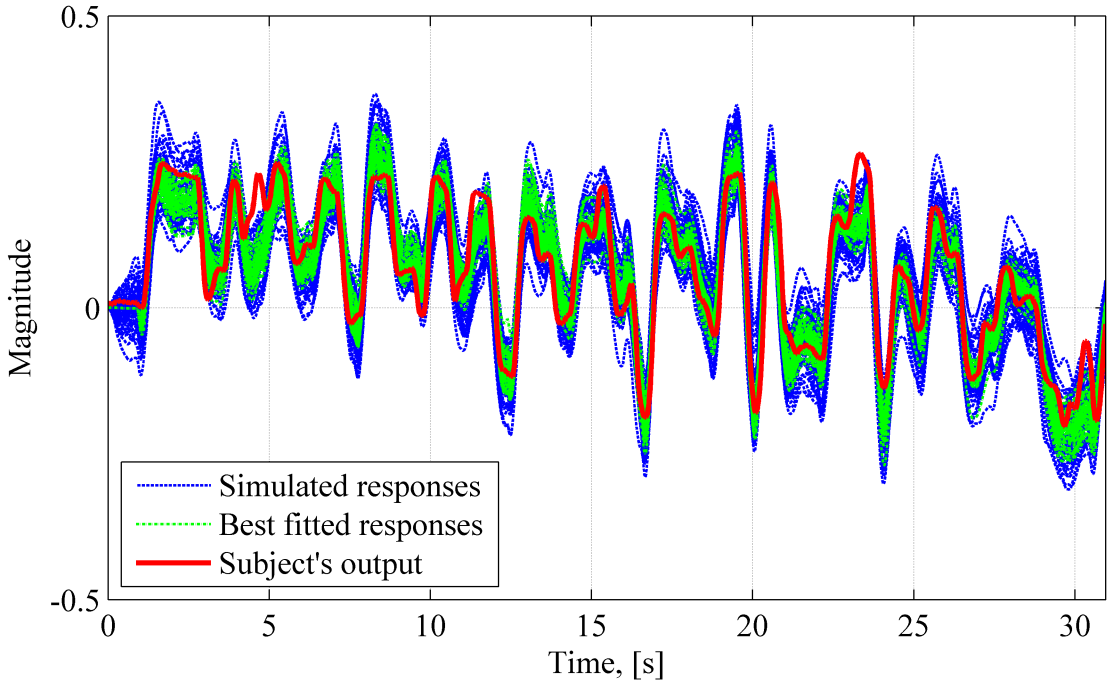

Figure 7: Input and output data collected from subject 1 and the response of the estimated model.

advantage of structured uncertainties the criterion of determining whether a dynamical system is robustly stable with respect to its uncertainties can be formulated in terms of a structured singular value μ. With the μ value a dynamical system is said to be robustly stable if and only if the following condition is satisfied (see Theorem 10.7 in [Zhou and Doyle, 1998])

$$\sup_{\omega\in\mathbb{R}} \mu_{\Delta_{st}}(G(j\omega)) \leq \beta, \tag{8}$$

with $\beta > 0$ such that $\|\Delta_{st}\|_\infty < 1/\beta$, where the μ value is defined as follows.

$$\mu_{\Delta_{st}}(G) = \frac{1}{\min\{\bar{\sigma}(\Delta_{st}) : \det(I - G\Delta_{st}) = 0\}}. \tag{9}$$

The value of $1/\mu$ has a physical meaning of the smallest perturbation that makes the generalized plant $G(s)$ unstable. Therefore, μ has been used as a measure of system's robustness.

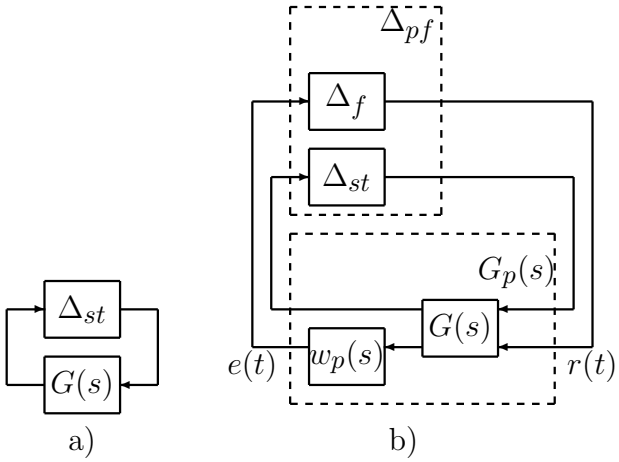

Figure 8: Robust tests diagrams: a) robust stability test, b) robust performance test.

The robust stability of a dynamical system is an important question; however, the real goal of the analysis and control design is to satisfy predefined performance characteristics. It is possible that a system is internally stable, but it performs poorly. Thereby, the robust performance analysis has to be involved. The robust performance analysis answers the question whether or not a dynamical system meets (or has a good performance) desired performance specifications. The diagram for the robust performance test is presented in Fig. 8 b) and as it can be noticed the robust performance test is transformed to the robust stability test with $G(s)$ combined with a performance weighting function $w_p(s)$ into the weighted generalized plant $G_p(s)$, and Δ_{st} combined with Δ_f into Δ_{pf} as follows.

$$\Delta_{pf} = \begin{bmatrix} \Delta_{st} & 0 \\ 0 & \Delta_f \end{bmatrix}, \tag{10}$$

where Δ_f is the fictitious uncertainty matrix, which characterizes the disturbance input, and $w_p(s)$ is the performance weighting function, which establishes the desired performance objective. With this formulation, a good robust performance means that the generalized plant $G_p(s)$ with the disturbance input $r(t)$ and the error output $e(t)$ (see Fig. 8 b) and Fig. 9) is robustly stable with respect to a set of all uncertainties specified

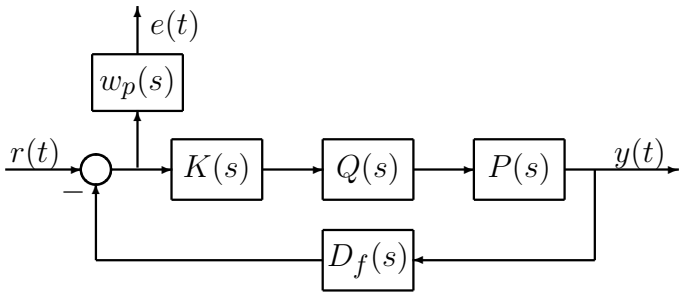

Figure 9: Head-neck system model with performance scaling.

for that dynamical system in Δ_{pf}.

In terms of the μ value, an uncertain dynamical system is said to have good robust performance if the following condition is satisfied

$$\sup_{\omega \in \mathbb{R}} \mu_{\Delta_{pf}}(G_p(j\omega)) \leq \beta, \tag{11}$$

where $\beta > 0$ such that $\|\Delta_{pf}\|_\infty < 1/\beta$. It is also clear that robust performance implies robust stability but not vice versa. The performance of a MIMO dynamical systems could be characterized in terms of $\mathcal{H}_\infty$ norm of the sensitivity function that is the transfer function from the input $r(t)$ to the output $e(t)$, as shown in Fig. 9. The robust performance criterion using the sensitivity function can be specified as follows.

$$\|S\|_\infty \leq \beta, \Delta_{pf} \in \mathcal{RH}_\infty, \|\Delta_{pf}\|_\infty < 1/\beta, \tag{12}$$

where $S(s)$ is the "weighted" sensitivity function defined as follows.

$$S(s) = \bar{S}(s) w_p(s), \text{ where } \bar{S}(s) = \frac{1}{1 + K(s)Q(s)P(s)D_f(s)}. \tag{13}$$

The performance weighting function $w_p(s)$ is described using parameters $A, B, \omega_b,$ and q as follows.

$$w_p(s) = \frac{(s/B^{1/q} + \omega_b)^q}{(s + \omega_b A^{1/q})^q}, \tag{14}$$

where parameters of $w_p(s)$ are chosen such as $A = 1.0$, $B = 4.0$, $w_b = 0.01$ Hz, and $q = 20.0$. Note that the choice of the performance weighting function is not restricted to the form presented in Eq. (14). In this form $w_p(s)$ acts as a weighting function, which suppresses the magnitude of the sensitivity function $\bar{S}(j\omega)$ in the frequency range above ω_b and amplifies it over the frequency range below ω_b. The parameters A and B define suppression/amplification levels and the parameter q is used to make the transition between two frequency ranges more narrow. Mathematically, the effect of the $w_p(s)$ on the $\mathcal{H}_\infty$ norm of the sensitivity function $\bar{S}$ can be shown as follows.

$$\begin{aligned} & |\bar{S}(j\omega)| \leq \frac{1}{|w_p(j\omega)|} \\ \Leftrightarrow\ & |\bar{S}(j\omega) w_p(j\omega)| \leq 1 \\ \Leftrightarrow\ & \|\bar{S} w_p\|_\infty \leq 1, \text{for } \forall\ \omega \in \mathbb{R} \\ \Leftrightarrow\ & \|S\|_\infty \leq 1 \end{aligned} \tag{15}$$

The performance weighting function provides a flexible way to define performance specifications for the robust performance analysis of the head-neck system. An appropriate choice of the form and parameters of $w_p(s)$ that reflects a performance boundary between subjects in control and pain groups can be used to classify subjects. The difference between value of $\|S\|_\infty$ and 1 may be related to the likelihood for a particular subject to be injured and a classification criterion with an appropriate choice of $w_p(s)$ can be determined such that

$$\begin{aligned} &\|S\|_\infty \leq 1, \text{for } \forall\ \omega \in \mathbb{R},\ \text{then the performance specification is met,} \\ &\|S\|_\infty > 1, \text{for } \forall\ \omega \in \mathbb{R},\ \text{then the performance specification is not met.} \end{aligned} \tag{16}$$

Uncertain block	Subj. 1	Subj. 2	Subj. 3	Subj. 4	Subj. 5
$K(s)$	1.554	1.149	1.058	1.176	1.754
$Q(s)$	$< 10^{-3}$	$< 10^{-3}$	$< 10^{-3}$	$< 10^{-3}$	$< 10^{-3}$
$P(s)$	0.893	0.882	0.699	0.769	0.997
$D_f(s)$	0.943	0.916	0.996	0.930	1.215

Table 1: μ values for the robust stability analysis with respect to uncertainties in the head-neck system model blocks.

Uncertain block	Subj. 1	Subj. 2	Subj. 3	Subj. 4	Subj. 5
$K(s)$	1.865	1.376	1.255	1.430	2.076
$Q(s)$	0.549	0.626	0.521	0.570	0.568
$P(s)$	0.957	0.924	0.746	0.792	1.060
$D_f(s)$	1.204	1.064	1.058	1.046	1.491

Table 2: μ values for the robust performance analysis with respect to uncertainties in the head-neck system model blocks.

5 Robust Analysis of the Head-neck System Components

In this chapter we provide the results of the μ analysis for the case when uncertainties exist in each individual block of the head-neck system. We are interested in determining which block with uncertainties (controller $K(s)$, muscle dynamics $Q(s)$, plant dynamics $P(s)$ or delay in the feedback channel $D_f(s)$) is most critical to robust stability and robust performance of the whole head-neck system. In order to do this, we consider that only one particular block has uncertainties while all other system's blocks are fixed at their nominal parameters. The computational results of the robust stability and robust performance tests for each individual uncertain block are presented in Table 1 for robust stability and in Table 2 for robust performance tests.

The highest μ value corresponds to the block of the closed-loop system which is most

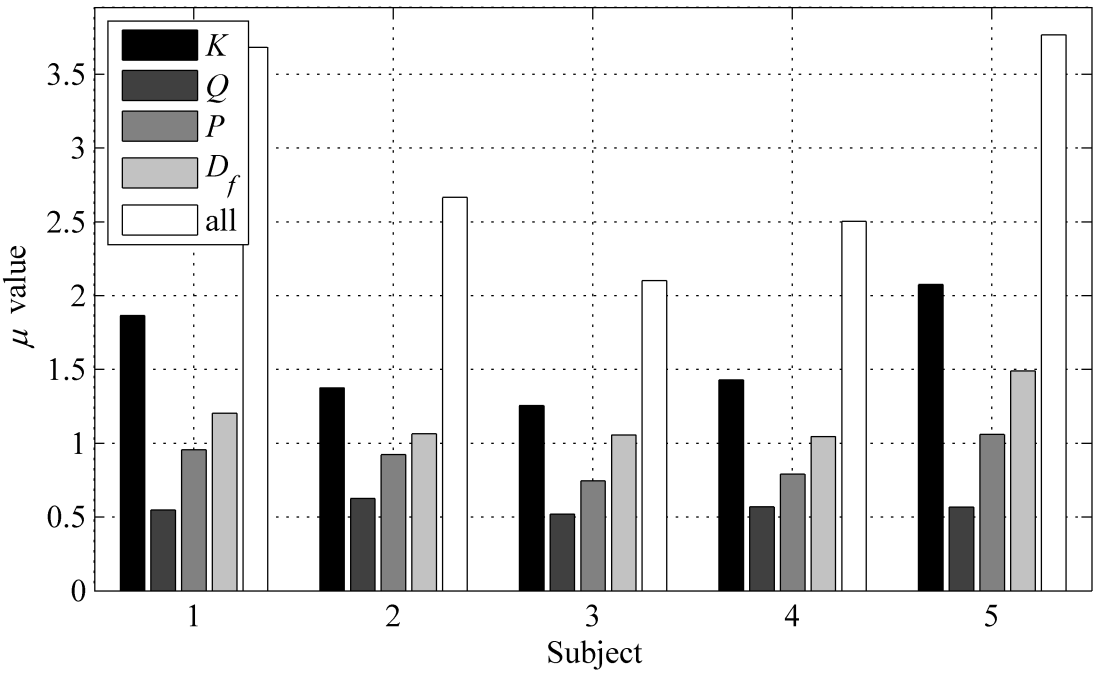

Figure 10: μ values for the robust performance analysis with respect to uncertainties in the head-neck system model blocks.

critical to system's stability and performance. We can notice that the computed μ values for different uncertain blocks for the robust stability as well as for the robust performance have approximately similar trends among all subjects.

For the robust stability case we can observe that the muscle dynamics block does not play a significant role; on the contrary, uncertainties in control block $K(s)$ are most crucial to robust stability of the head-neck system for all subjects. At the same time, uncertainties in plant dynamics and in the feedback delay affect robust stability approximately at the same level. We can see the same trends from the robust performance analysis. The illustration of μ values from the robust performance tests for all tested subjects presented in Fig. 10.

It is also interesting to note that all μ values for all considered cases for subject 5 is higher than for all other subjects. This correlates with our observation about the estimation variability of subject 5 that is higher than those of other subjects. It is also

Test	Subj. 1	Subj. 2	Subj. 3	Subj. 4	Subj. 5
Stability	3.344	2.450	1.917	2.265	3.405
Performance	3.683	2.666	2.102	2.503	3.766

Table 3: μ values for the robust stability and robust performance analyses with respect to all uncertainties.

interesting to compare μ values related to the whole uncertain head-neck system. As can be seen from Table 3 subject 5 has the highest μ values among others for both robust stability and robust performance tests. At the same time, the μ values for subject 3 are the smallest ones. In other words, subject 3 is the most robust subject, whereas subject 5 is the least robust among other subjects.

6 Individual Parametric Uncertainty Effect on Robust Stability and Performance

In this chapter we analyze how each individual uncertainty affects robust stability and robust performance of the head-neck system. To perform such analysis we assume that only one parameter of the system is uncertain. All other parameters are fixed at their nominal values. Results of robust stability and robust performance tests for each individual parameter are presented in Table 4 and Table 5, respectively.

The delay in the feedback channel is the almost primary parameter affecting robust stability of the system. This is essential from the feedback control point of view. For two subjects the analysis also shows that the integral gain may affect robust stability of the head-neck system.

More interesting observations can be made from the results for the robust performance tests. Delay in feedback still significantly influence system performance; however, depending on the subject it may not be the most crucial parameter. Control gains are now the

Parameter	Subj. 1	Subj. 2	Subj. 3	Subj. 4	Subj. 5
K_p	$< 10^{-3}$	$< 10^{-3}$	$< 10^{-3}$	$< 10^{-3}$	$< 10^{-3}$
K_d	$< 10^{-3}$	$< 10^{-3}$	$< 10^{-3}$	$< 10^{-3}$	$< 10^{-3}$
K_i	$< 10^{-3}$	$< 10^{-3}$	0.897	$< 10^{-3}$	$< 10^{-3}$
τ_m	$< 10^{-3}$	$< 10^{-3}$	$< 10^{-3}$	$< 10^{-3}$	$< 10^{-3}$
I	$< 10^{-3}$	$< 10^{-3}$	$< 10^{-3}$	$< 10^{-3}$	$< 10^{-3}$
b	$< 10^{-3}$	$< 10^{-3}$	$< 10^{-3}$	$< 10^{-3}$	$< 10^{-3}$
k	$< 10^{-3}$	$< 10^{-3}$	$< 10^{-3}$	$< 10^{-3}$	$< 10^{-3}$
τ_f	0.943	0.916	0.996	0.930	1.215

Table 4: μ values for the robust stability analysis with respect to individual uncertainty.

Parameter	Subj. 1	Subj. 2	Subj. 3	Subj. 4	Subj. 5
K_p	1.261	1.144	0.904	1.111	1.190
K_d	1.696	0.917	0.732	0.869	1.959
K_i	0.971	1.000	0.930	0.909	1.080
τ_m	0.549	0.626	0.521	0.570	0.568
I	0.463	0.379	0.359	0.374	0.502
b	0.911	0.740	0.739	0.694	1.042
k	0.881	0.870	0.713	0.783	0.966
τ_f	1.204	1.064	1.058	1.046	1.491

Table 5: μ values for the robust performance analysis with respect to individual uncertainty.

most influential. The parameters of plant dynamics could also affect robust performance of the system significantly but according to μ values their impact on system's performance is slightly less than those of control block parameters.

It seems that uncertainties in muscle dynamics and in inertia of the plant are less important for robust performance of the head-neck system. However, the corresponding μ values are not too small to neglect parameters τ_m and I of these blocks.

7 Worst-case Performance Analysis

Worst-case analysis provides us with the system parameters that lead to the worst-case performance. The procedure of computing such worst-case parameters was developed in [Shin et al., 2001] with an application to the X-38 crew return vehicle. In the application to the head-neck system computation of the worst-case scenario, we want to determine a vector of parameters θ_{wc} such that the magnitude of the sensitivity function $S(\theta_{wc}, s)$ is highest over the whole set of possible models defined by the subject's variability Θ_{subj}. Mathematically this problem can be defined as follows.

$$\theta_{wc} = \underset{\theta \in \Theta_{subj}}{\arg\max} \; \|S(j\omega)\|_\infty. \tag{17}$$

The worst-case analysis is of interest since it shows the worst-performance of a tested subject with that specific combination of parameters computed from the analysis. Assuming that physiological problems with the subject's plant dynamics can be independent from the rest of the system dynamics, we investigate three worst-case scenarios. The first scenario (denoted as $KQPD_f$ WC) is related to the worst-case of the whole head-neck system with uncertainties in all parameters. In the second scenario (KQD_f WC) only uncertainties in the control block, muscle dynamics and the delay in the feedback channel are considered. Finally, the worst-case scenario of only the plant dynamics is considered (P WC).

In terms of robust control, the worst-case is defined as the magnitude peak of the sensitivity function (weighted sensitivity in general) of a system. The critical frequency f_{cr} and the magnitude corresponding to this peak. Consequently, our interest is not only to compute the parameters of the system that lead to the worst-case scenario, but also to identify the corresponding frequency at this magnitude peak. Values of $\|S\|_\infty$ are computed as lower and upper bounds. The upper bound is of interest. The parameters

WC Scenario	Subj. 1	Subj. 2	Subj. 3	Subj. 4	Subj. 5
$KQPD_f$	0.010	0.113	0.085	0.120	0.010
KQD_f	0.056	0.209	0.195	0.230	0.064
P	1.111	1.510	1.618	1.232	0.015

Table 6: Worst-case critical frequencies.

WC Scenario	Subj. 1	Subj. 2	Subj. 3	Subj. 4	Subj. 5
$KQPD_f$	inf	Inf	Inf	Inf	Inf
KQD_f	Inf	Inf	Inf	Inf	Inf
P	-2.44	-4.20	-6.86	-6.21	9.42

Table 7: Worst-case $\|S\|_\infty$ values.

that lead to the worst-case scenario are related to the lower bound case, but the infinite upper bound is related to the case when magnitude peak is sharp and the computation of the exact value of $\|S\|_\infty$ is problematic. The critical frequencies f_{cr} are listed in Table 6 as well as the magnitudes of the peak $\|S\|_\infty$ are in Table 7.

The computed worst-case parameters are listed in Table 12 in Appendix B. A couple of observations can be made using this table for the worst-case scenarios $KQPD_f$ and KQD_f. The proportional gain K_p for all subject tends to be the smallest value within the subject's variability. The integral gain K_i tends to increase (except subjects 1 and 5 in $KQPD_f$ worst-case scenario) but not necessarily up to the upper bound within subject's total variability. At the same time, the derivative gain K_p values are not consistent. The values of the delay time constant τ_f and the parameter τ_m of the muscle dynamics block are maximal within individual subject's variability. There is no strong consistency in the worst-case parameters of the plant dynamics block.

Other observations from the worst-case analyses can be made from Tables 6 and 7. First, the worst-case scenarios $KQPD_f$ and KQD_f primary occur at frequencies below 0.3 Hz. In addition, the critical frequency for the worst-case scenario $KQPD_f$ is smaller

than that of KQD_f. For subjects 1 and 5 f_{cr} for the worst-case scenarios $KQPD_f$ tends to zero. At the same time, the worst-case scenario P occurs at frequencies above 1.0 Hz, which significantly distinguish this worst-case scenario from two others.

The magnitude peaks for the worst-case scenarios $KQPD_f$ and KQD_f are sharp and the upper bound of the $\|S\|_\infty$ is infinity. However, the magnitude peaks of the worst-case scenario P are smooth and the corresponding values of the $\|S\|_\infty$ are finite. In addition, the $\|S\|_\infty$ value for subject 5 is higher than 0 dB and for other subjects this values are less than 0 dB. This means that the worst-case scenario P for subjects 1, 2, 3, and 4 is still satisfy performance specifications.

Finally, the illustration of the frequency responses of the sensitivity functions, including worst-case sensitivity functions, is presented in Figs. 12, 14, 16, 18, and 20 in Appendix B as well as the simulated time responses of the head-neck system model with the worst-case parameters in Figs. 13, 15, 17, 19, and 21. Parameters of the head-neck system model that lead to the worst-case are listed in Table 12 of Appendix.

8 Robust Control Design

In this chapter we present results of the optimally (or suboptimally) synthesized robust controller for the head-neck system. The synthesized robust controller could help in planning rehabilitation. The robust controller is designed using the nonsmooth optimization, which has to be involved due to the structural constraints (PID structure in our case) imposed on the controller. In our case, this procedure is a search of a combination of the controller gains K_p, K_d, and K_i (within the subject's variability) that minimizes the $\mathcal{H}_\infty$ norm of the sensitivity function $S(j\omega)$. Mathematically, this problem is formulated as follows.

$$k := \arg\min_{k\in\mathcal{K}} \|S(j\omega, \theta, k)\|_\infty, \tag{18}$$

Par.	Subj. 1		Subj. 2		Subj. 3		Subj. 4		Subj. 5	
	Nom.	Tuned	Nom.	Tuned	Nom.	Tuned	Nom.	Tuned	Nom.	Tuned
K_p	0.287	0.116	0.923	0.196	0.890	0.196	0.835	0.179	0.180	0.089
K_d	0.196	0.048	0.263	0.056	0.359	0.066	0.241	0.054	0.235	0.044
K_i	0.030	0.000	0.115	0.000	0.083	0.061	0.096	0.042	0.048	0.000

Table 8: Parameters of the tuned robust controller of the head-neck system.

where k is a vector that contains the controller gains (K_p, K_d, and K_i), and $\mathcal{K}$ is a closed set prescribed by the parameter-wise variabilities of those control gains from Θ_{subj}.

In particular the nonsmooth $\mathcal{H}_\infty$ synthesis proposed by [Apkarian and Noll, 2006] and [Bruisma and Steinbuch, 1990] is used, which is an effective way to solve a non-convex $\mathcal{H}_\infty$ synthesis problem where controller is subject to structural constraints.

The results are presented in Table 8.

The computed robust control gains are smaller rather than the estimated control gains. In general, smaller control gains mean that robust control is less aggressive in comparison to the estimated control. Another interesting observation is that the integral gain K_i in the robust controller tends to be the smallest value within subjects' variability. These tendencies can be clearly seen in Fig. 11.

9 Conclusions

In this dissertation we proposed a new methodology of measuring robustness of the head-neck system. This methodology is based on performing the robust stability and robust performance analyses of the head-neck system with respect to uncertainties. Uncertainties come from the biological variability of the parameters of the system and from the estimation errors. The robust stability and robust performance tests provide us with the μ value that may be used as an objective measure in clinical evaluation.

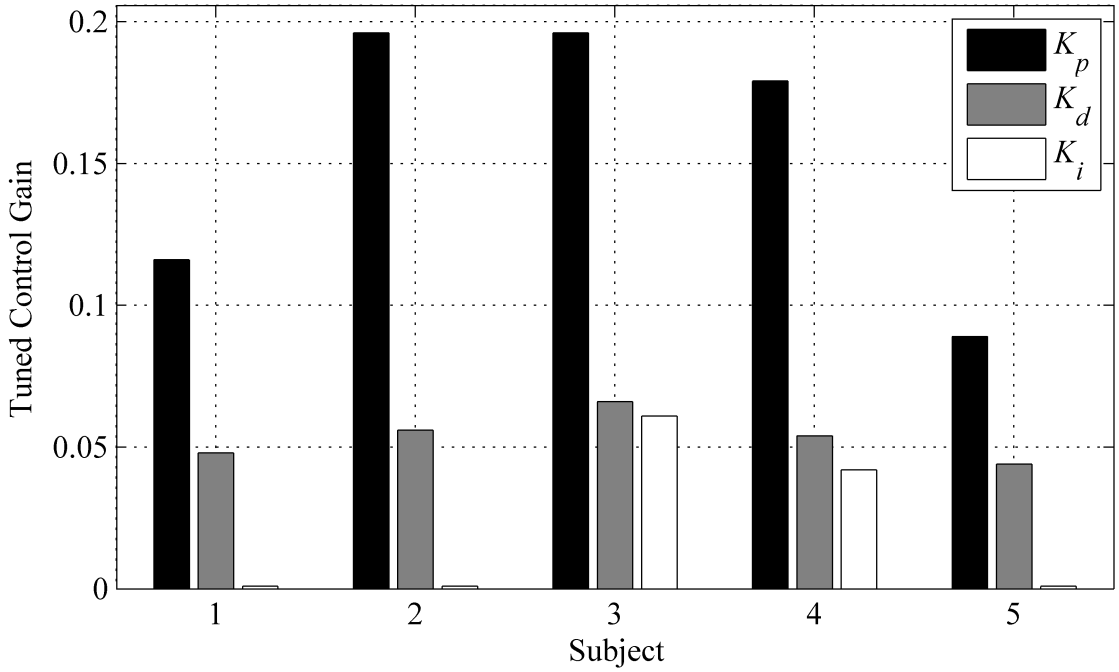

Figure 11: Robust control design. Tuned control gains.

The general procedure for our approach can be summarized as follows:

1. Determine the biological variability of a subject via estimating a parametric model using subject's responses during position tracking experiments.

2. Determine the estimation variability of the dynamical model for a subject by analyzing estimation error statistics.

3. Determine the total variability as the union of the biological and estimation variabilities.

4. Perform robust analyses of the system including robust stability and robust performance tests.

5. Perform the worst-case performance analysis of the system.

6. Design an optimal (or suboptimal) robust controller for planning rehabilitation.

We also applied our methodology using the experimental data collected with five adult subjects. Using the experimental data we showed that the estimated parameters and variabilities for the four subjects have a trend and the simulated responses are very close to the actual subjects' responses. Our experimental setup allows us to capture dynamics of the head-neck system. Subject 5 was exceptional showing relatively large modeling errors.

The robust analysis of each individual uncertain block of the head-neck system showed a strong trend in the μ values for different blocks among tested subjects.

In the robust analysis of each individual uncertainty we noted that robust stability of the system was affected by the delay in the feedback channel and for some subjects by the integral gain of the PID controller. In the case of robust performance, all individual uncertainties affected system's performance. The control gains and delays in feedback are more crucial; however, uncertainties in plant dynamics as well as in the muscle dynamics block cannot be neglected.

With the worst-case analysis we can clearly see that the worst-case scenario for the whole system occurs at frequencies below 0.150 Hz and the worst-case scenario with uncertainties in control, muscle dynamics and delays in feedback only occurs in frequencies within range from 0.150 to 0.300. At the same time, the worst-case scenario, in the case when uncertainties exist in the plant only, occurs at frequencies above 1 Hz and its peak has finite value.

The designed robust control design showed the tendencies that the control gains of the robust controller are smaller than those of the estimated nominal system. In other words, the robust controller tends to be less aggressive. The synthesized robust controller could help in planning rehabilitation.

APPENDICES

A Estimated Parameters and Subject Variabilities

In this Appendix we provide tables with the estimated parameter values and determined subject's biological and total variabilities. Parameters of the control block are listed in Table 9, parameters of the plant and muscle dynamics blocks are in Table 10 and the delay time constants are listed in Table 11.

		K_p	K_d	K_i
Subj. 1	Nominal value	0.287	0.196	0.030
	Bio. variability	[0.087, 0.562]	[0.130, 0.401]	[0.000, 0.142]
	Total variability	[0.000, 1.406]	[0.057, 1.365]	[0.000, 0.591]
Subj. 2	Nominal value	0.923	0.263	0.115
	Bio. variability	[0.404, 1.304]	[0.232, 0.317]	[0.000, 0.502]
	Total variability	[0.274, 3.543]	[0.111, 0.904]	[0.000, 3.828]
Subj. 3	Nominal value	0.890	0.359	0.083
	Bio. variability	[0.320, 1.584]	[0.210, 0.784]	[0.000, 0.236]
	Total variability	[0.180, 2.981]	[0.096, 1.143]	[0.000, 1.617]
Subj. 4	Nominal value	0.835	0.241	0.096
	Bio. variability	[0.431, 1.117]	[0.202, 0.355]	[0.000, 0.399]
	Total variability	[0.241, 3.136]	[0.073, 0.903]	[0.000, 1.371]
Subj. 5	Nominal value	0.180	0.235	0.048
	Bio. variability	[0.033, 0.402]	[0.102, 0.474]	[0.000, 0.146]
	Total variability	[0.000, 1.355]	[0.085, 7.225]	[0.000, 1.587]

Table 9: Subjects' variabilities and parameters of the nominal system. Control block

		τ_m	I	b	k
Subj. 1	Nominal value	0.229	0.025	0.158	0.030
	Bio. variability	[0.097, 0.500]	[0.024, 0.026]	[0.107, 0.261]	[0.006, 0.122]
	Total variability	[0.050, 0.500]	[0.024, 0.026]	[0.100, 0.916]	[0.000, 0.424]
Subj. 2	Nominal value	0.148	0.033	0.228	0.073
	Bio. variability	[0.123, 0.186]	[0.032, 0.035]	[0.100, 0.282]	[0.006, 0.209]
	Total variability	[0.050, 0.500]	[0.032, 0.035]	[0.100, 0.643]	[0.000, 0.998]
Subj. 3	Nominal value	0.168	0.032	0.191	0.079
	Bio. variability	[0.105, 0.420]	[0.031, 0.034]	[0.100, 0.302]	[0.014, 0.224]
	Total variability	[0.050, 0.500]	[0.031, 0.034]	[0.100, 0.712]	[0.000, 0.466]
Subj. 4	Nominal value	0.160	0.027	0.176	0.074
	Bio. variability	[0.128, 0.217]	[0.026, 0.029]	[0.100, 0.223]	[0.022, 0.182]
	Total variability	[0.050, 0.500]	[0.026, 0.029]	[0.100, 0.536]	[0.000, 0.591]
Subj. 5	Nominal value	0.230	0.029	0.125	0.030
	Bio. variability	[0.050, 0.500]	[0.028, 0.031]	[0.100, 0.239]	[0.000, 0.090]
	Total variability	[0.050, 0.500]	[0.028, 0.031]	[0.100, 5.281]	[0.000, 1.493]

Table 10: Subjects' variabilities and parameters of the nominal system. Muscle and plant dynamics

		τ_i	τ_f
Subj. 1	Nominal value	0.181	0.135
	Bio. variability	[0.155, 0.209]	[0.000, 0.447]
	Total variability	[0.130, 0.258]	[0.000, 0.500]
Subj. 2	Nominal value	0.188	0.039
	Bio. variability	[0.165, 0.207]	[0.000, 0.064]
	Total variability	[0.152, 0.247]	[0.000, 0.237]
Subj. 3	Nominal value	0.150	0.011
	Bio. variability	[0.133, 0.171]	[0.000, 0.036]
	Total variability	[0.116, 0.181]	[0.000, 0.194]
Subj. 4	Nominal value	0.177	0.024
	Bio. variability	[0.158, 0.189]	[0.000, 0.045]
	Total variability	[0.140, 0.211]	[0.000, 0.186]
Subj. 5	Nominal value	0.192	0.106
	Bio. variability	[0.155, 0.244]	[0.000, 0.285]
	Total variability	[0.108, 0.362]	[0.000, 0.500]

Table 11: Subjects' variabilities and parameters of the nominal system. Delays

B Worst-case Analysis Numerical Results and Plots

In this Appendix we present the numerical results for the worst-case analysis of the head-neck system. The computed worst-case parameter values are listed in Table 12. The magnitude plots of the worst-case sensitivity functions are shown in Figs. 12, 14, 16, 18, and 20. The corresponding simulated responses of the worst-case head-neck system models are shown in Figs. 13, 15, 17, 19, and 21.

		Nominal	KQD_fP WC	KQD_f WC	P WC
Subj. 1	K_p	0.287	0.004	0.000	nominal
	K_d	0.196	0.623	0.946	nominal
	K_i	0.030	0.006	0.141	nominal
	τ_m	0.229	0.500	0.500	nominal
	b	0.158	0.916	nominal	0.100
	k	0.030	0.001	nominal	0.424
	τ_f	0.135	0.500	0.500	nominal
Subj. 2	K_p	0.923	0.274	0.274	nominal
	K_d	0.263	0.111	0.121	nominal
	K_i	0.115	0.337	0.515	nominal
	τ_m	0.148	0.500	0.500	nominal
	b	0.228	0.643	nominal	0.100
	k	0.073	0.000	nominal	0.998
	τ_f	0.039	0.237	0.237	nominal
Subj. 3	K_p	0.890	0.180	0.180	nominal
	K_d	0.359	1.012	0.805	nominal
	K_i	0.083	0.476	1.469	nominal
	τ_m	0.168	0.500	0.500	nominal
	b	0.191	0.712	nominal	0.100
	k	0.079	0.000	nominal	0.466
	τ_f	0.011	0.194	0.194	nominal
Subj. 4	K_p	0.835	0.241	0.241	nominal
	K_d	0.241	0.073	0.505	nominal
	K_i	0.096	0.311	1.352	nominal
	τ_m	0.160	0.500	0.500	nominal
	b	0.176	0.536	nominal	0.100
	k	0.074	0.000	nominal	0.000
	τ_f	0.024	0.186	0.186	nominal
Subj. 5	K_p	0.180	0.000	0.000	nominal
	K_d	0.235	0.085	0.641	nominal
	K_i	0.048	0.021	0.126	nominal
	τ_m	0.230	0.500	0.500	nominal
	b	0.125	5.281	nominal	5.281
	k	0.030	0.027	nominal	0.000
	τ_f	0.106	0.500	0.500	nominal

Table 12: Worst-case parameter values of the head-neck system.

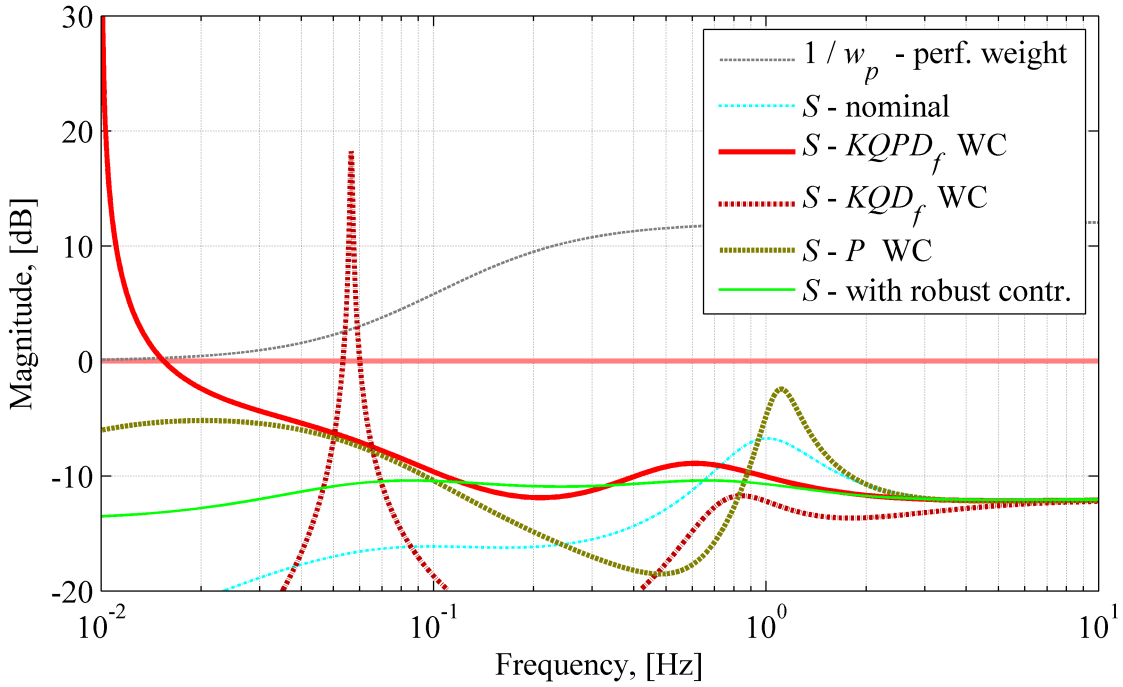

Figure 12: Magnitude plot of the sensitivity functions. Subject 1.

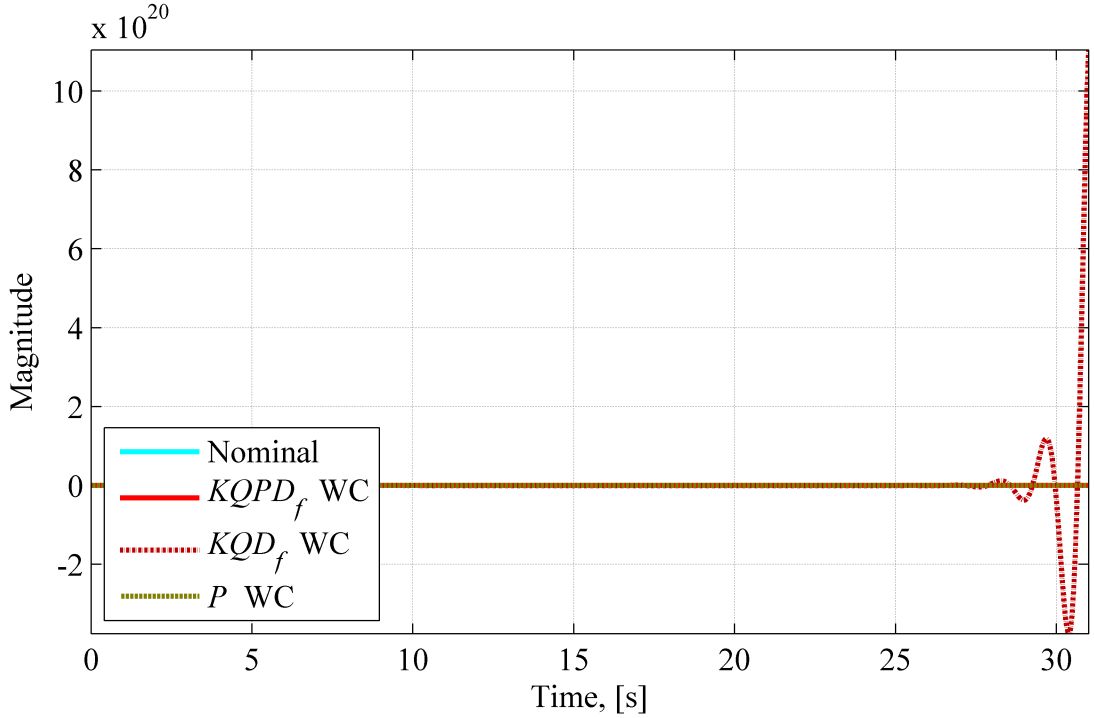

Figure 13: Simulated responses of the worst-case head-neck system models. Subject 1.

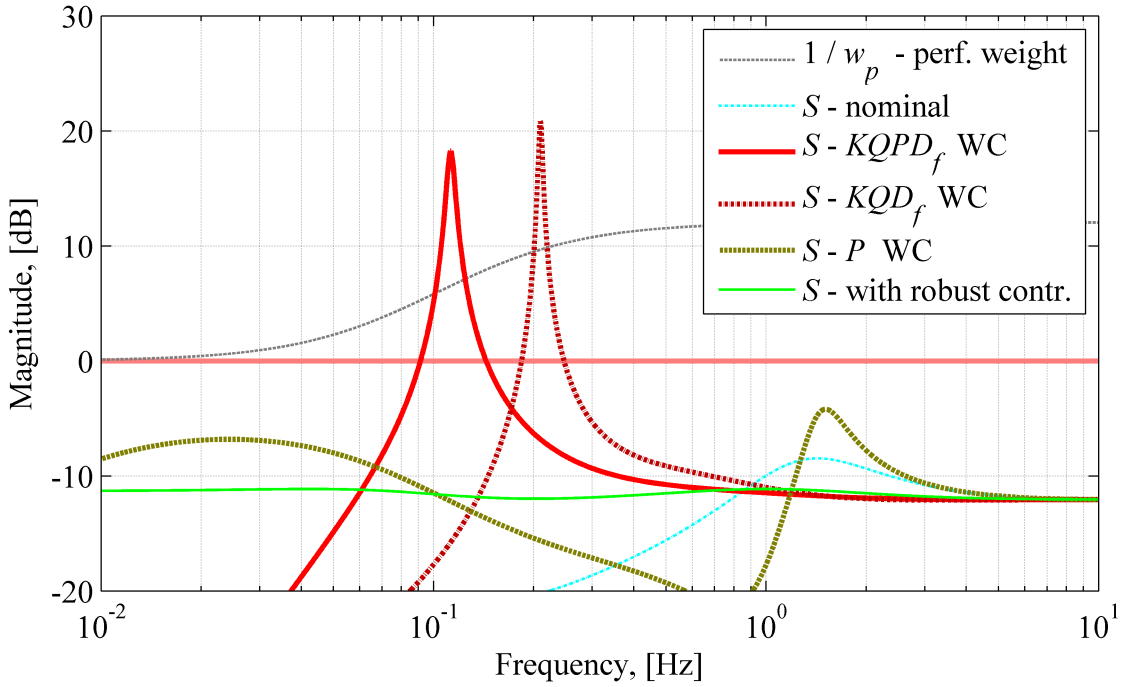

Figure 14: Magnitude plot of the sensitivity functions. Subject 2.

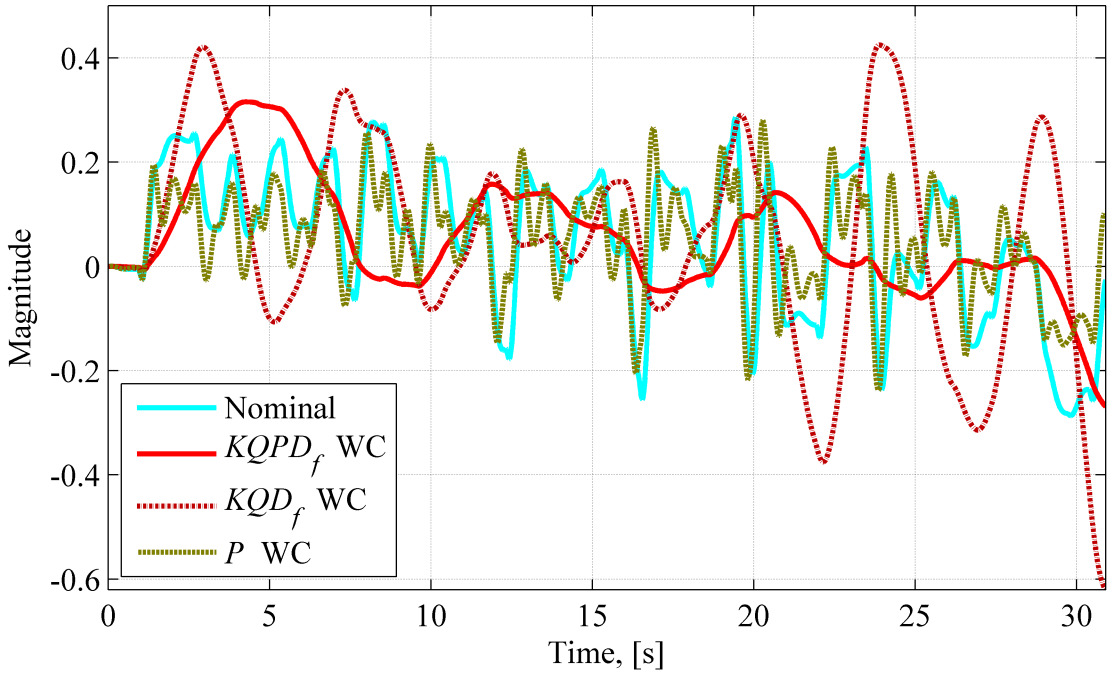

Figure 15: Simulated responses of the worst-case head-neck system models. Subject 2.

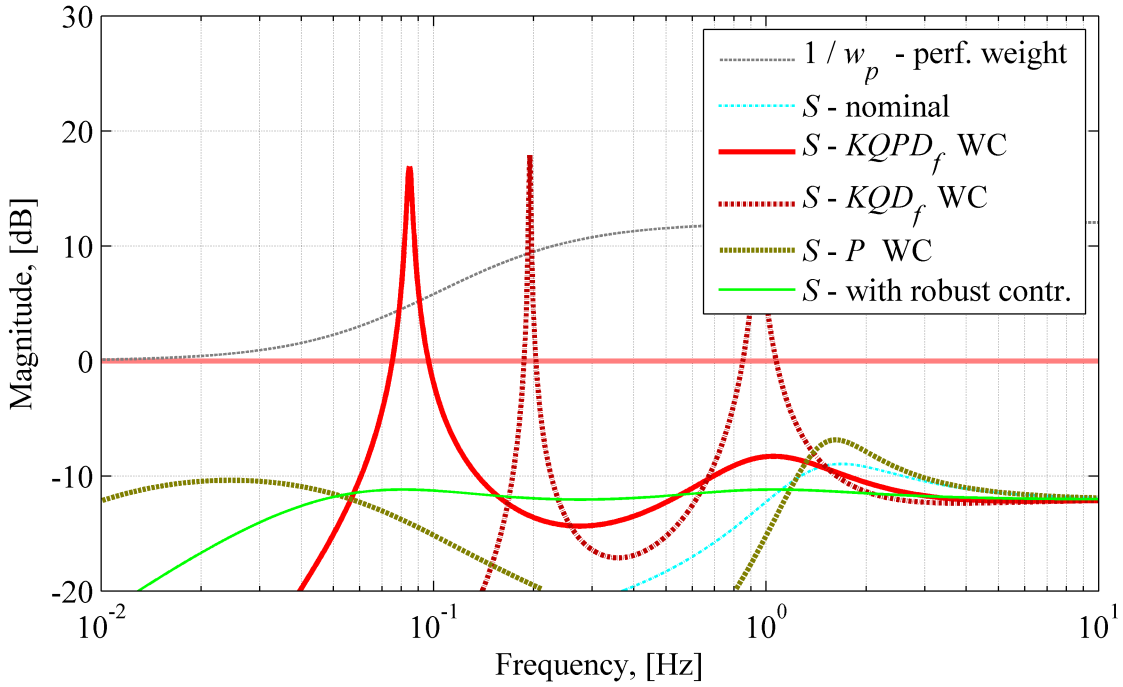

Figure 16: Magnitude plot of the sensitivity functions. Subject 3.

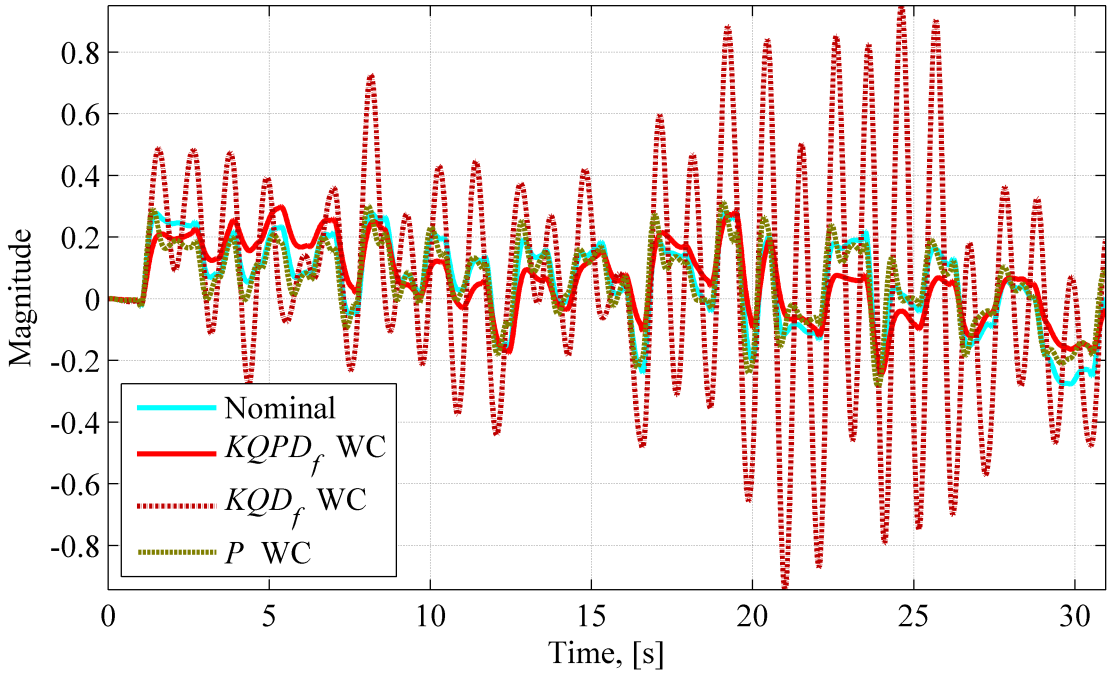

Figure 17: Simulated responses of the worst-case head-neck system models. Subject 3.

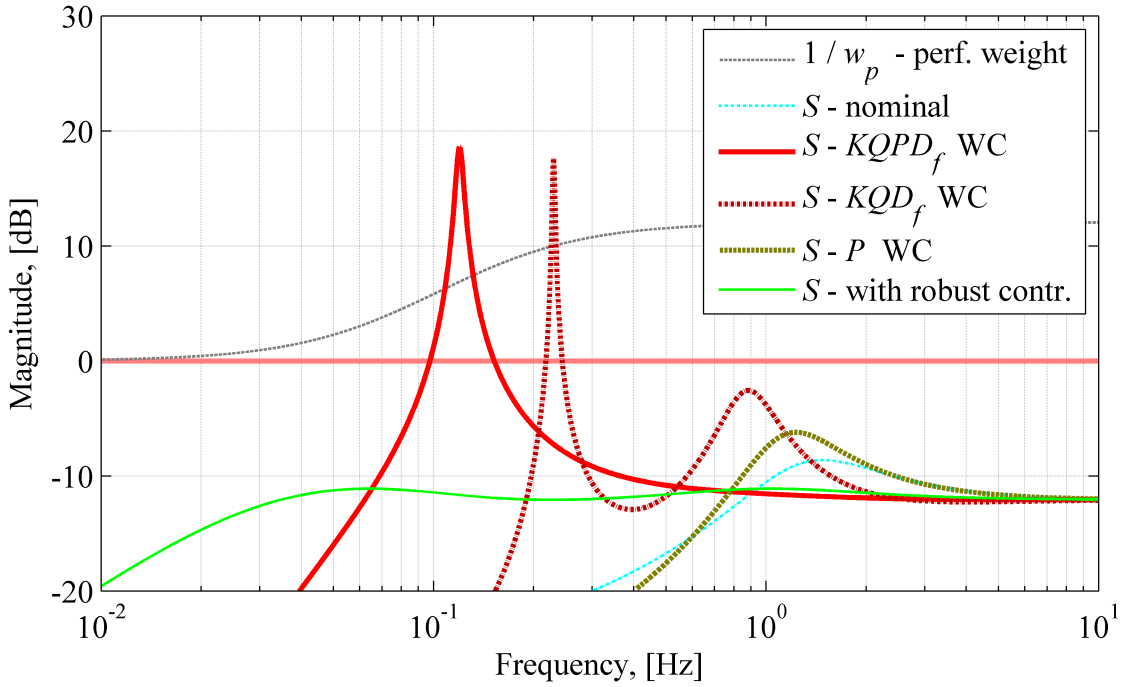

Figure 18: Magnitude plot of the sensitivity functions. Subject 4.

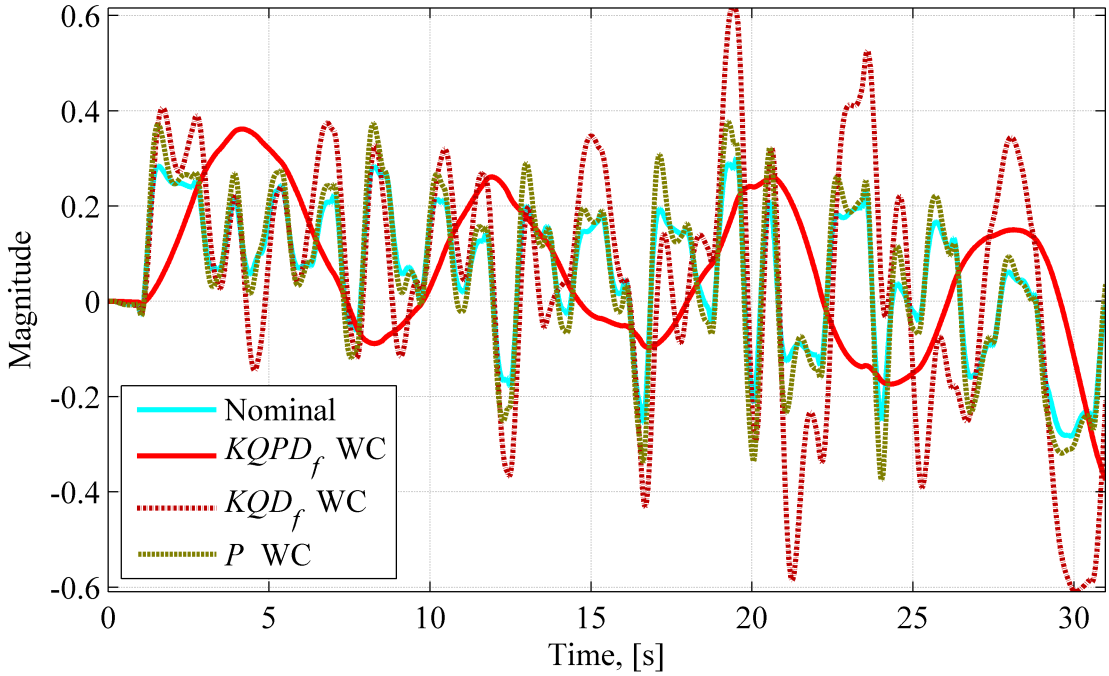

Figure 19: Simulated responses of the worst-case head-neck system models. Subject 4.

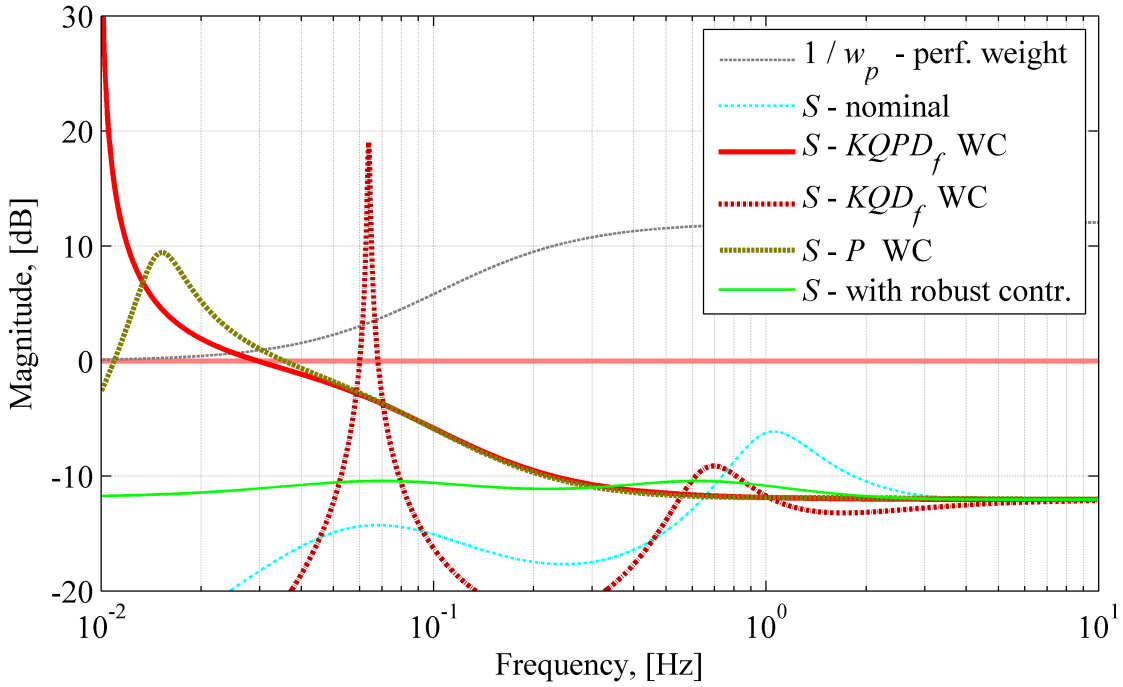

Figure 20: Magnitude plot of the sensitivity functions. Subject 5.

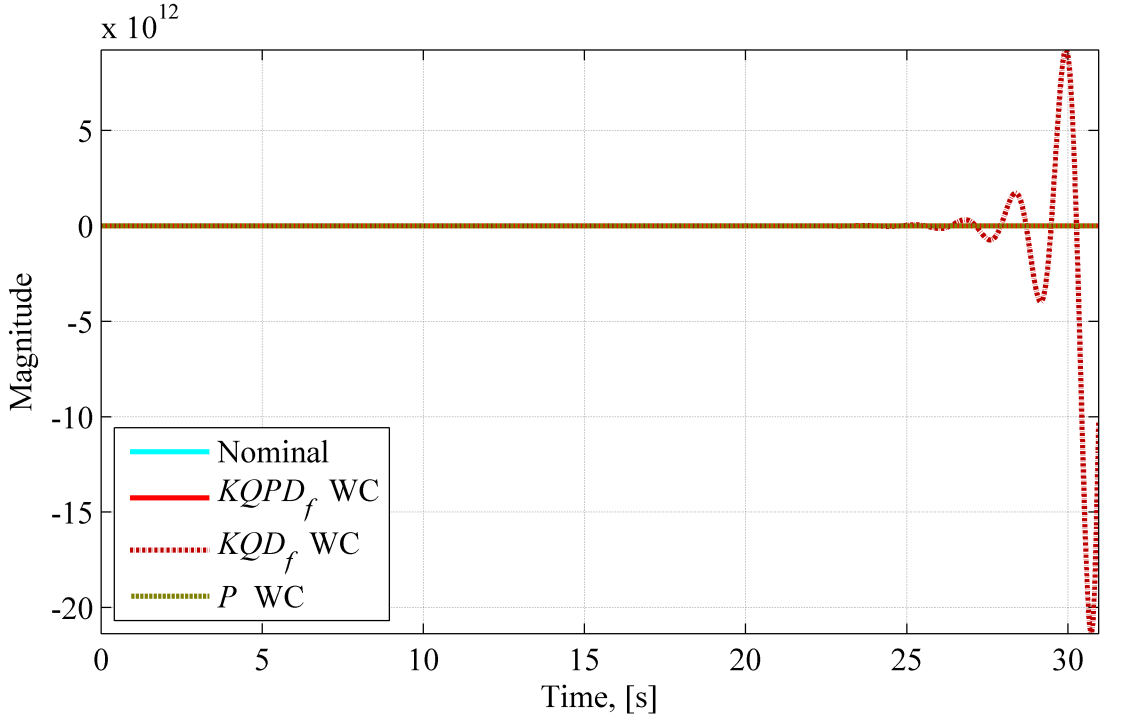

Figure 21: Simulated responses of the worst-case head-neck system models. Subject 5.

REFERENCES

REFERENCES

P. Apkarian and D. Noll. Non-smooth H-infinity synthesis. *IEEE Transactions on Automatic Control*, 51(1):71–86, 2006.

G. J. Balas, J. C. Doyle, K. Glover, A. Packard, and R. Smith. *μ-Analysis and Synthesis Toolbox For Use with MatLAB*, 2001.

G. J. Balas, R. Chiang, A. Packard, and M. Safonov. *Robust Control Toolbox for Use with MatLAB*, 2006.

X. Bombois. *Connecting Prediction Error Identification and Robust Control Analysis: a new framework*. PhD thesis, PhD thesis. Université Catholique de Louvain. Louvain-la-Neuve, Belgium, 2000.

X. Bombois, M. Gevers, G. Scorletti, and B. D. Anderson. Robustness analysis tools for an uncertainty set obtained by prediction error identification. *Automatica*, 37(10): 1629–1636, 2001.

N. Bourdet and R. Willinger. Coupled headâĂŞneckâĂŞtorso and seat model for car seat optimization under rear-end impact. *Journal of Sound and Vibration*, 313(3):891–907, 2008.

N. A. Bruisma and M. Steinbuch. A fast algorithm to compute the H_∞-norm of a transfer function matrix. *System & Control Letters*, 14(4):287–293, 1990.

J. R. Carl and R. S. Gellman. Human smooth pursuit: stimulus-dependent responses. *Journal of Neurophysiology*, 57(5):1446–1463, 1987.

K. J. Chen, E. A. Keshner, B. W. Peterson, and T. C. Hain. Modeling head tracking of visual targets. *Journal of Vestibular Research*, 12(1):25–33, 2002.

P. Côté, J. D. Cassidy, and L. Carroll. The saskatchewan health and back pain survey. the prevalence of neck pain and related disability in saskatchewan adults. *Spine*, 23 (15), 1998.

K. Davids, S. Bennett, and K. M. Newell. *Movement System Variability*. Human Kinetics 1, 2006.

J. E. Dennis Jr. Nonlinear least-squares. *State of the Art in Numerical Analysis*, pages 269–312, 1977.

U. Forssell and L. Ljung. Closed-loop identification revisited. *Automatica*, 35(7):1215–1241, 1999.

M. Gevers, X. Bombois, B. Codrons, G. Scorletti, and B. Anderson. Model validation for control and controller validation in a prediction error identification approach - part i : theory. *Automatica*, 39(3):403–415, 2003.

I. Gustavsson, L. Ljung, and T. Söderström. Identification of processes in closed loop - identifiability and accuracy aspects. *Automatica*, 13(1):59–75, 1977.

B. Hannaford, W. S. Kim, S. H. Lee, and L. Stark. Neurological control of head movements. inverse modeling and electromyographic evidence. *Mathematical Biosciences*, 78 (2):159–178, 1986.

E. Holmström, J. Lindell, and U. Moritz. Low back and neck/shoulder pain in construction workers: occupational workload and psychosocial risk factors. part 2: Relationship to neck and shoulder pain. *Spine*, 17(6), 1992.

W. P. Huebner, R. J. Leigh, S. H. Seidman, C. W. Thomas, C. Billian, A. O. DiScenna, and L. F. Dell'osso. Experimental tests of a superposition hypothesis to explain the relationship between the vestibuloocular reflex and smooth pursuit during horizontal combined eye-head tracking in humans. *Journal of Neurophysiology*, 68(5):1775–1792, 1992.

P. Hur, B. A. Duiser, S. M. Salapaka, and E. T. Hsiao-Wecksler. Measuring robustness of the postural control system to a mild impulsive perturbation. *IEEE Transactions on Neural Systems and Rehabilitation Engineering*, 18(4):461–467, 2010.

G. B. Langley and H. Sheppeard. The visual analogue scale: its use in pain measurement. *Rheumatology international*, 5(4):145–148, 1985.

K. Levenberg. A method for the solution of certain problems in least-squares. *Quarterly of Applied Math*, (2):164–168, 1944.

L. Ljung. *System Identification*. Wiley Online Library, second edition, 1999.

D. W. Marquardt. An algorithm for least-squares estimation of nonlinear parameters. *Journal of the Society for Industrial & Applied Mathematics*, 11(2):431–441, 1963.

K. Masani, A. H. Vette, and M. R. Popovic. Controlling balance during quiet standing: Proportional and derivative controller generates preceding motor command to body sway position observed in experiments. *Gait & Posture*, 23(2):164–172, 2006.

K. M. Newell and D. M. Corcos. *Variability and motor control*. Human Kinetics, 1993.

S. Pankoke, B. Buck, and H. P. Woelfel. Dynamic FE model of sitting man adjustable to body height, body mass and posture used for calculating internal forces in the lumbar vertebral disks. *Journal of Sound and Vibration*, 215(4):827–839, 1985.

G. C. Peng, B. W. Peterson, and T. Hain. A dynamical model for reflex activated head movements in the horizontal plane. *Biological Cybernetics*, 75(4):309–319, 1996.

B. W. Peterson, H. Choi, T. Hain, E. Keshner, and G. C. Y. Peng. Dynamic and kinematic strategies for head movement control. *Annals of the New York Academy of Sciences*, 942(1):381–393, 2001.

M. C. Priess, C. J. Radcliffe, and J. Choi. Application of real-time image distortion compensation to a ïňĄrearm simulation environment. *Proceedings of 2010 ASME Dynamic Systems and Control Conference (DSCC)*, pages 13–15, 2010.

M. C. Priess, J. M. Popovich, J. Choi, N. P. Reeves, J. Cholewicki, and C. J. Radcliffe. The importance of delay location in modeling the human head-neck target tracking system. *MSU Technical Report*, 2012.

J. G. Reber and W. Goldsmith. Analysis of large head-neck motions. *Journal of Biomechanics*, 12(3):211–222, 1979.

D. A. Robinson, J. L. Gordon, and S. Gordon. A model of the smooth pursuit eye movement system. *Biological Cybernetics*, 55(1):43–57, 1986.

J.-Y. Shin, G. J. Balas, and A. K. Packard. Worst-case analysis of the X-38 crew return vehicle flight control system. *Journal of Guidance, Control, and Dynamics*, 24(2):261–269, 2001.

S. Skogestad and I. Postlethwaite. *Multivariable Feedback Control: Analysis and Design*. Wiley, second edition, 2005.

A. H. Vette, T. Yoshida, T. A. Thrasher, K. Masani, and M. R. Popovic. A complete, non-lumped, and verifiable set of upper body segment parameters for three-dimensional dynamic modeling. *Medical Engineering & Physics*, 33(1):70–79, 2011.

D. A. Winter. *Biomechanics and motor control of human movement*. Wiley, 2004.

Y. Xu, J. Choi, N. P. Reeves, and J. Cholewicki. Optimal control of the spine system. *Journal of Biomechanical Engineering*, 132(5), 2010.

N. Yoganandan, F. A. Pintar, J. Zhang, and J. L. Baisden. Physical properties of the human head: Mass, center of gravity and moment of inertia. *Journal of Biomechanics*, 42(9):1177–1192, 2009.

K. Zhou and J. C. Doyle. *Essentials of Robust Control*. Prentice-Hall, 1998.